Photodynamic Properties of Azobenzene Molecular Films with Triphenylamines

Mi-Jeong Kim, Eun-Mi Seo, Doojin Vak, and Dong-Yu Kim*

Center for Frontier Materials, Department of Materials Science and Engineering, Kwangju Institute of Science and Technology (K-JIST), 1 Oryong-dong, Buk-gu, Kwangju 500-712, Republic of Korea

Received March 28, 2003. Revised Manuscript Received July 17, 2003

A new type of photochromic molecule containing three azobenzene groups, tris[(4-(phenylazo)diphenylamine) phenylamine] (TPPA), was synthesized and its photoinduced behavior was examined. Good optical quality TPPA films could be prepared by spin-coating. The photoinduced behavior of the TPPA films, such as photoinduced birefringence and surface relief grating (SRG) formation, was investigated. Compared to an azobenzene-functionalized polymeric PDO3 film, the TPPA molecular film showed a rapid response for photoinduced birefringence and SRG formation, but the saturated value for the birefringence was much smaller than that of the PDO3 azopolymer film. The dynamic behavior of SRG photofabrication was compared for two TPPA films with different morphologies: an amorphous film prepared by spin coating and a semicrystalline film prepared by vacuum thermal deposition. The crystallinity associated with the TPPA film strongly hampered photoinduced mass transport in the fabrication of SRG.

1. Introduction

Low molecular weight organic glass film has been a subject of extensive study in various research fields. Organic films with a glass transition temperature (T_g) well above room temperature are required for use in optics, electronics, and optoelectronics applications.[1] However, molecular films have a tendency to undergo crystallization. To obtain an amorphous molecular glass and to control the T_g, major structural factors such as molecular flexibility, steric hindrance, and intermolecular interaction must be controlled. An amorphous molecular glass can be constructed in the form of nonstackable odd-shaped molecules or as twin molecules where bulky groups are linked via flexible or semi-flexible central groups.[2] Typically, the structural units used in glass-forming molecules are spiro-,[3] tetrahedral-,[4] and starburst-shapes,[5,6] including a triphenylamine family.[7,8]

The photoinduced linear orientation of the azobenzene groups in polymer films has been widely known for more than a decade. When such a film is irradiated with a linearly polarized laser beam, the azobenzene groups become oriented perpendicular to the incident polarization direction of the light via the trans−cis−trans photoisomerization cycles.[9−11] However, the extent of our knowledge of photoinduced orientation of azobenzenes in the case of *molecular films* is limited. Their behavior could be quite different from that of polymer films. It was also reported, in 1995, that a surface relief grating (SRG) with submicron periodic structures could be photofabricated on the surface of azobenzene functionalized polymer films using holographic interference patterns of laser beams.[12−14] Since then, a number of studies have been directed at exploring a process for potential applications and to better understand the detailed mechanism.[15−20] SRG formation is not clearly understood currently, but is believed to occur by polymer chain migration resulting from trans−cis−trans pho-

* To whom correspondence should be addressed. Tel: +82-62-970-2319. Fax: +82-62-970-2304. E-mail: kimdy@kjist.ac.kr.

(1) Shirota, Y. *J. Mater. Chem.* **2000**, *10*, 1.
(2) Alig, I.; Braun, D.; Langendorf, R.; Wirth, H. O.; Voigt, M.; Wendorff, J. H. *J. Mater. Chem.* **1998**, *8*, 847.
(3) Salbeck, J.; Yu, N.; Bauer, J.; Weissörtel, F.; Bestgen, H. *Synth. Met.* **1997**, *91*, 209.
(4) Robinson, M. R.; Wang, S.; Bazan, G. C.; Cao, Y. *Adv. Mater.* **2000**, *12*, 1701.
(5) Adachi, C.; Tsutsui, T.; Saito, S. *Appl. Phys. Lett.* **1990**, *56*, 799.
(6) Kuwabara, Y.; Ogawa, H.; Inada, H.; Noma, N.; Shirota, Y. *Adv. Mater.* **1994**, *6*, 677.
(7) Shirota, Y.; Moriwaki, K.; Yoshikawa, S.; Ujike, T.; Nakano, H. *J. Mater. Chem.* **1998**, *8*, 2579.
(8) Utsumi, H.; Nagahama, D.; Nakano, H.; Shirota, Y. *J. Mater. Chem.* **2000**, *10*, 2436.
(9) Meng, X.; Natansohn, A.; Barrett, C.; Rochon, P. *Macromolecules* **1996**, *29*, 946
(10) Natansohn, A.; Rochon, P. *Macromolecules* **1998**, *31*, 7960, and references therein.
(11) Ono, H.; Kowatari, N.; Kawatsuki, N. *Opt. Mater.* **2001**, *17*, 387.
(12) Rochon, P.; Batalla, E.; Natansohn, A. *Appl. Phys. Lett.* **1995**, *66*, 136.
(13) Kim, D. Y.; Tripathy, S. K.; Li, L.; Kumar, J. *Appl. Phys. Lett.* **1995**, *66*, 1166.
(14) Kim, D. Y.; Li, L.; Jiang, X. L.; Shivshankar, V.; Kumar, K.; Tripathy, S. K. *Macromolecules* **1995**, *28*, 8835.
(15) Jiang, X. L.; Li, L.; Kumar, J.; Kim, D. Y.; Shivshankar, V.; Tripathy, S. K. *Appl. Phys. Lett.* **1996**, *68*, 2618.
(16) Viswanathan, N. K.; Kim, D. Y.; Bian, S.; Williams, J.; Liu, W.; Li, L.; Samuelson, L.; Kumar, J.; Tripathy, S. K. *J. Mater. Chem.* **1999**, *9*, 1941.
(17) Kumar, J.; Li, L.; Jiang, X. L.; Kim, D. Y.; Lee, T. S.; Tripathy, S. *Appl. Phys. Lett.* **1998**, *72*, 2096.
(18) Barrett, C. J.; Rochon, P. L.; Natansohn, A. L. *J. Chem. Phys.* **1998**, *109*, 1505.
(19) Pedersen, T. G.; Johansen, P. M.; Holme, N. C. R.; Ramanujam, P. S. *Phys. Rev. Lett.* **1998**, *80*, 89.
(20) Sumaru, K.; Yamanaka, T.; Fukuda, T.; Matsuda, H. *Appl. Phys. Lett.* **1999**, *75*, 1878.

10.1021/cm034207d CCC: $25.00
Published on Web 09/25/2003

toisomerization cycles of the azobenzene groups. In most cases, such studies have focused on SRG formation on polymeric films owing to the ease of the amorphous film formation by the spin-casting process.

Compared to a polymer, molecular glasses would be expected to provide better defined molecular systems that are free from polymer chains and their entanglement, and have a high density of azobenzene groups even though polymers containing only azobenzene chromophores have been synthesized using azo-phenols.[21] Recently, the photofabrication of a SRG was also demonstrated on the case of a molecular glass with azobenzene groups.[22−24] Our research group reported that a molecular glass could be prepared using an isocyanate-based cyclic molecule containing azobenzenes.[23] We have shown that with nearly identical compositions SRG formation was more efficient on the trimer molecular film than on the polymer film due to a decrease in chain entanglement. It has also been reported that triphenylamine-based azo glass films possess SRG formation capability.[22,24] However, a detailed comparison of photoinduced properties, such as optically induced birefringence and SRG formation, between a molecular glass and a polymer film has not been reported to date. A detailed study of this relationship would play an important role in our understanding of the response of azobenzene-functionalized materials to light.

Organic thin films can be prepared by various techniques, e.g., solvent cast from solution, spin-coating, electrochemical deposition, Langmuir−Blodgett, and self-assembly methods.[1] The properties of the molecular films, especially the morphology, are strongly dependent on the film processing conditions even though the materials used are the same.[1] The photodynamic SRG formation process on azobenzene molecular films will be greatly affected by the morphology of the film because this process is believed to be a mass transport process. Therefore, organic molecular films can be a good material system in which the mechanism of photodynamic behaviors of azobenzene materials could be examined using their various morphological states.

In this study, we report on the synthesis of a new azobenzene-functionalized triphenylamine molecule, tris[(4-(phenylazo)diphenylamine)phenylamine] (TPPA). The TPPA molecule contains three azobenzene groups, which was the highest density of azobenzene groups among molecular glasses reported to date[7,22,24] and shows a good film-forming capability by both spin coating and vacuum evaporation methods. In the first part of this paper, photoinduced birefringence and SRG formation on TPPA molecular films are described and the results are compared to the known characteristics of an azobenzene polymer PDO3 film.[13−17] In the second part, crystalline TPPA films prepared by vacuum vapor deposition and their photoinduced SRG formation are described and compared to that for an amorphous TPPA molecular glass.

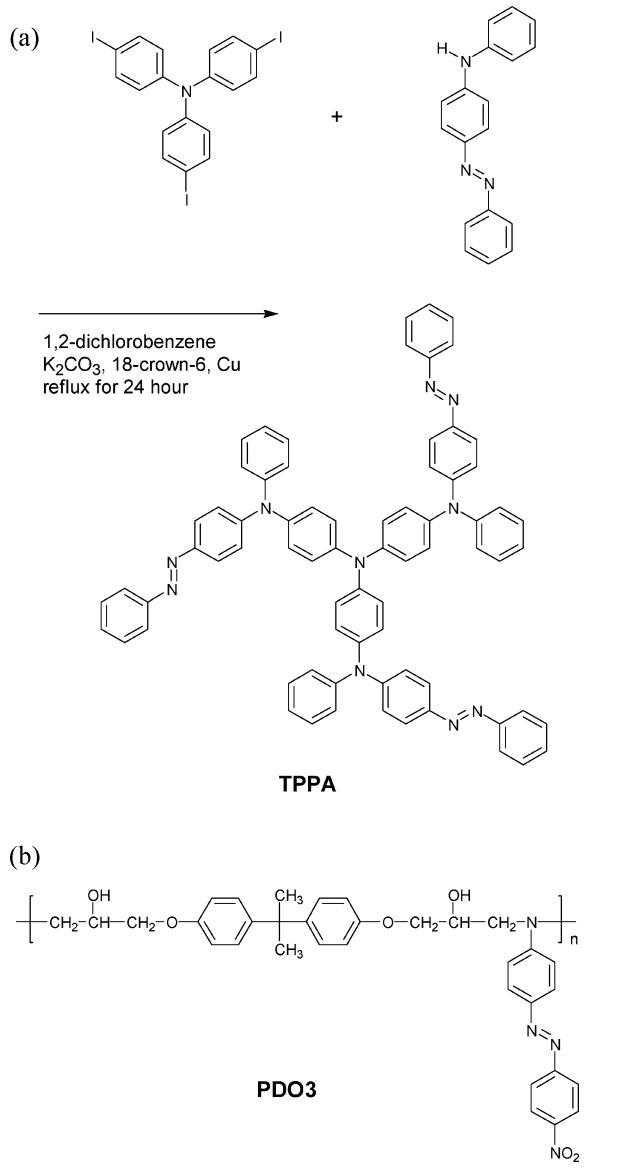

Figure 1. (a) Synthetic scheme and chemical structure for the triphenylamine-based azobenzene molecule, tris[(4-(phenylazo)diphenylamine)phenylamine] (TPPA), and (b) chemical structure of the epoxy-based amorphous azobenzene polymer, poly(disperse orange 3) (PDO3).

2. Experimental Section

2.1. Material Synthesis. The synthetic scheme for the photochromic azobenzene-functionalized molecule, tris[(4-(phenylazo)diphenylamine) phenylamine] (TPPA), is shown in Figure 1a. Tris(iodophenylamine) was purchased from TCI and all other reagents were purchased from Aldrich Chemicals; all were used without further purification. Tris(iodophenylamine), 4-(phenylazo)diphenylamine (or Disperse Orange 1), potassium carbonate, and copper as catalyst were mixed in 1,2-dichlorobenzene and stirred at 190 °C under reflux (Ullman coupling reaction).[25] After a 24 h reaction, the mixtures were cooled, filtered, and washed with water, 2 N NaOH, and a dilute HCl solution. The filtered solution was dried with magnesium sulfate. Methanol was added to the reaction mixture and the precipitate was dried under vacuum. The pure product was separated by column chromatography using hexane/methylenchloride 1:3 as the eluent. The product was dried under a vacuum at 70 °C for 12 h.

The yield was about 80%. ^{1}H NMR ($CDCl_3$, 300 MHz) δ (ppm): 7.8−7.71 (phenylazo, ortho position, *p*-azophenylamine,

(21) Tripathy, S. K.; Kim, D. Y.; Li, L.; Viswanathan, N. K.; Balasubramanian, S.; Liu, W.; Wu, P.; Bian, S.; Samuelson, L.; Kumar, J. *Synth. Met.* **1999**, *102*, 893.
(22) Fuhrmann, T.; Tsutsui, T. *Chem. Mater.* **1999**, *11*, 2226.
(23) Seo, E.-M.; Kim, M. J.; Shin, Y.-D.; Lee, J.-S.; Kim, D.-Y. *Mol. Cryst. Liq. Cryst.* **2001**, *370*, 143.
(24) Nakano, H.; Takahashi, T.; Kadota, T.; Shirota, Y. *Adv. Mater.* **2002**, *14*, 1157.
(25) Gauthier, S.; Frechet, J. M. J. *Synthesis* **1987**, 383.

inner position, 12H), 7.4−7.3 (phenylazo, para, and metha position, 9H), 7.2−7.1 (phenylamine, ortho, and metha position, 12H), 7.06−7.01 (phenylamine, para position, *p*-azophenylamine, outer position, diamine-phenyl, 21H). Poly(disperse orange 3) (PDO3) was synthesized from diglycidyl ether of bisphenol A and disperse orange 3 following the literature procedure,[26] and recrystallized using tetrahydrofuran and methanol.

2.2. Film Preparation Methods. Amorphous TPPA films were prepared using 8 wt % TPPA in 1,1,2,2-tetrachloroethane solution, and amorphous PDO3 films were prepared using 8 wt % PDO3 polymer in a cyclohexanone solution by a spin-coating process. All the films were baked under a vacuum above the T_g for 12 h. The thickness of the films was varied from 200 to 1000 nm depending on the spinning speed (600−2500 rpm). TPPA films were also prepared by vacuum thermal evaporation method at a pressure of 1.2×10^{-6} Torr. TPPA films with two different thicknesses (150 and 300 nm) were also prepared by vacuum thermal evaporation for comparison.

2.3. Photofabrication of SRG. Experiments dealing with the holographic fabrication of SRGs on azobenzene-functionalized films were performed using an interference pattern of Ar^+ laser beams at a wavelength of 488 nm with 50−100 mW/cm^2 intensity. The linear polarized light of the Ar^+ laser beam was passed through a half-waveplate in order to set a p-polarization state for the light source. It was then expended and collimated by a spatial filter and a lens. Half of the collimated beam was directly incident on the film and the other portion of the beam was reflected from an aluminum-coated mirror onto the film.[15] The incident angle of the light source was 14 degrees, which corresponds to a 1-μm grating spacing determined by Bragg conditions ($\lambda = 2d\sin\theta$, where λ is wavelength, d is period of interference pattern, and θ is incident angle). The growth rate of the diffraction efficiency was monitored by its first-order diffraction from a 1.2-mW He−Ne laser beam with s-polarization at 633 nm in the transmission mode.

2.4. Characterizations. The photochromic materials were identified by ^{1}H NMR (JEOL JNM-LA 300 WB FT-NMR) spectroscopy, in a deuterated chloroform solution. Thermal properties, such as glass transition temperature (T_g) and melting temperature (T_m) of the TPPA and PDO3 powders (after purification by chromatography and recrystallization) were characterized using differential scanning calorimetry (DSC, DSC2100, TA instrument). This measurement was carried out in a nitrogen atmosphere with a scan rate of 10 °C/min. The film thickness was measured using an α-step surface profiler. The UV−Vis absorption spectra of the TPPA and PDO3 films were recorded from 350 to 700 nm with a Perkin Elmer Lambda spectrophotometer. Photoinduced birefringence was measured using an Ar^+ laser beam at 488 nm with 50 mW/cm^2 as a pump beam and a He−Ne laser with at 633 nm as a probe beam. The optical setup and the detailed procedures for the measurement of the optically induced birefringence have been described previously.[9−11] The crystallinity of the TPPA film prepared by vacuum vapor deposition was measured by X-ray diffraction measurements (Rigaku Co., Cu Kα radiation). Surface images and depth profiles of the prepared SRGs were measured by atomic force microscopy (AFM, Autoprobe CP, PSI) with a contact mode.

3. Results and Discussion

3.1. Comparison of Optically Induced SRGs between Molecular Glass and Polymer Films. A triphenylamine-based azobenzene molecule, TPPA, was successfully synthesized using the Ullman coupling reaction as shown in Figure 1a. The TPPA molecule has a very high density of photochromic units, that is, three azobenzene groups per molecule. The TPPA molecule has a radial shape and a nonplanar structure due to aromatic tertiary amine moieties. The TPPA molecule is not a rigid triangular structure. The TPPA molecule could have various conformers due to rotation of nitrogen−benzene bonds and inversion of four amines. The conformation shown in Figure 1a is one of those conformers, and the most stable conformation calculated by semiempirical calculation using PM3 wave function in CAChe 5.0 work system. When the molecules were exposed to light, the photoisomerization of the azobenzene groups in the sidearms could occur independently. Therefore, the geometrical symmetry could be broken more easily under the irradiation leading to preferential orientation of the azobenzene groups. Figure 1b shows the chemical structure of an epoxy-based azopolymer, PDO3. The photoinduced formation of SRGs of the PDO3 was extensively studied by Tripathy and coworkers (including authors of this paper).[13−17,26] The polymer has several advantages such as a high content of azobenzene groups, a highly amorphous morphology, and an easy synthetic procedure. Figure 2 shows DSC thermograms of the TPPA molecule and the PDO3 polymer. The TPPA indicated the presence of both glassy and crystalline states (T_g = 80 °C, T_m = 220 °C). The synthesized PDO3 polymer has a T_g around 110 °C, but no T_m was observed, confirming that PDO3 is an amorphous polymer.

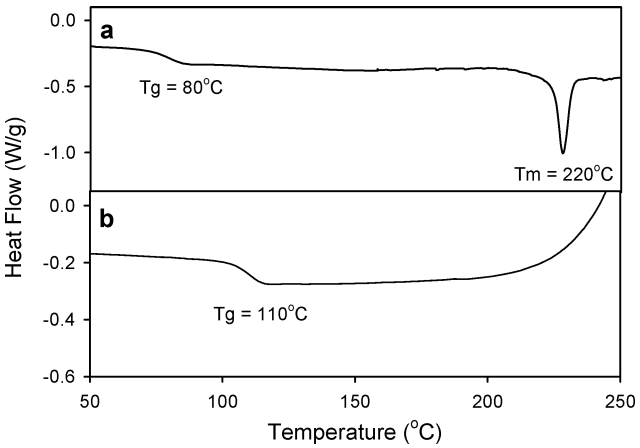

Figure 2. DSC thermograms of (a) TPPA and (b) PDO3 with a second scan.

Both TPPA and PDO3 films could be prepared by a spin-coating process. Both films showed amorphous morphology and good optical qualities with negligible scattering, which was also confirmed by polarized optical microscopy. In the case of TPPA, even though it has a semicrystalline nature, the nonplanar and randomly branched structure of the TPPA molecule made it possible to prepare a transparent and amorphous film by spin-coating. Figure 3 shows UV−Vis spectra of these films with a thickness of about 500 nm. The maximum absorption wavelengths (λ_{max}) of the TPPA and the PDO3 films were 445 and 460 nm, respectively. The PDO3 film showed higher λ_{max} due to the presence of nitro groups.

A well-known property of azo polymer films is the photoinduced linear orientation when the film is irradiated with a linearly polarized laser beam.[9−11] The azobenzene groups become oriented perpendicular to the incident polarization direction of the light through the trans−cis−trans photoisomerization cycle. These prop-

(26) Mandal, B. K.; Jeng, R. J.; Kumar, J.; Tripathy, S. K. *Makromol. Chem., Rapid Commun.* **1991**, *12*, 607.

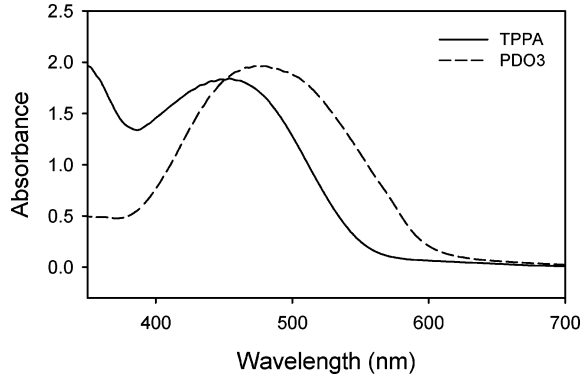

Figure 3. UV−Vis spectra of the TPPA (−) and the PDO3 (- - -) films with 500-nm thickness. Absorption coefficients of the TPPA and PDO3 films were 3.1×10^4 and 3.9×10^4 cm^{-1} at 488 nm, respectively.

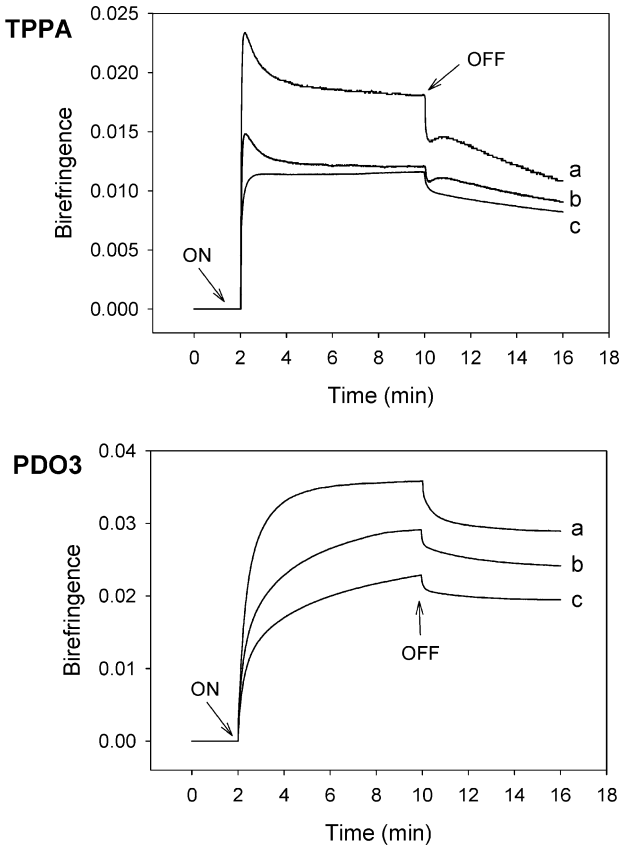

Figure 4. Photoinduced birefringence of the amorphous TPPA film and PDO3 films with film thicknesses of (a) 350 nm, (b) 500 nm, and (c) 1000 nm. The light source, a linear polarized Ar^+ laser with a 50 mW/cm^2 intensity, was turned on at $t = 2$ min and turned off at $t = 10$ min. The birefringence was further monitored for a 6-min relaxation period in the dark.

erties of the polymer films have been extensively studied during the past decade, however, to date, there seems to be no report on the photoinduced orientation of the azobenzenes in the case of molecular films. The behaviors could be quite different from that of polymer films. Therefore, we measured the optically induced birefringence in the TPPA films and compared them with those of the PDO3 film. For both TPPA and PDO3, three films with different thicknesses of 350, 500, and 1000 nm were prepared. The measured birefringence curves are shown in Figure 4 and the characteristics are summarized in Table 1.

Table 1. Photoinduced Birefringence Characteristics of the Amorphous TPPA and PDO3 Films

film thickness	saturation value	responsive time (min)[a]	remnant value[b]	remnant value (%)
		TPPA Film		
350	0.0182	< 0.03	0.0108	59
500	0.0121	< 0.05	0.0091	75
1000	0.0116	0.42	0.0082	71
		PDO3 Film		
350	0.0358	2.6	0.0289	81
500	0.0291	5.1	0.0242	83
1000	0.0229	6.1	0.0195	85

[a] Irradiation time required to reach 95% level of the saturated birefringence value. [b] Birefringence at $t = 16$ min. After the laser beam turned off at $t = 10$ min, thermal relaxation occurred during 6 min.

As the film thickness is increased, the saturated value and the response time for photoinduced birefringence gradually decreased probably due to less penetration of light on the thicker film due to absorption. When the two types of azo films with same thicknesses were compared, the PDO3 films showed about a two times larger value than that of the TPPA films. It has been reported that the photoinduced linear orientation of the azobenzene groups also leads to the linear orientation of the polymer main-chains through cooperative motions.[9] However, these types of cooperative effects would not be expected in the TPPA molecular films because of the lack of interconnecting backbone chains. For that reason, it is believed that azo molecular films could have a smaller value of photoinduced birefringence than that of azo polymer films.

The most interesting feature of the TPPA films is their rapid response to photoinduced birefringence, contrary to a gradual increase in the case of the PDO3 polymer film. When the linearly polarized Ar^+ laser beam was turned on, the birefringence of the TPPA film developed much faster than that of the PDO3 film. After only 12 s of irradiation of the TPPA film with a thickness of 350 nm, the birefringence instantly increased to a value of 2.34×10^{-2}. However, further irradiation with linear polarized light on the TPPA film led to a decrease in photoinduced birefringence, and finally, saturation at 1.82×10^{-2}. The reason for this unstable overshooting to occur at the very early exposure process is currently unclear. As the film thickness increased from 350 to 500 nm, this overshooting of photoinduced birefringence was reduced, and was not observed for the TPPA film with a thickness of 1000 nm. The response time, defined as the time required to reach a 95% level of the saturated birefringence value, was 0.42 min for the TPPA film with a thickness of 1000 nm, but 6.1 min for the PDO3 film. The absence of a polymer main-chain and its entanglement in the case of TPPA would permit the azobenzene groups to move freely and become rapidly oriented in the perpendicular direction where they absorb less linearly polarized light.

After the beam was turned off ($t = 10$ min in Figure 4), the relaxation of the induced birefringence was monitored in the dark. After 6 min, the remnant birefringence of the PDO3 film with a 1000 nm thickness was 85% of the level of the saturated value. However, the remnant birefringence was only 71% of the saturated value of the TPPA film with a 1000 nm thickness, and only 59% that of the TPPA film with a 350 nm thickness. Optically induced linear orientation

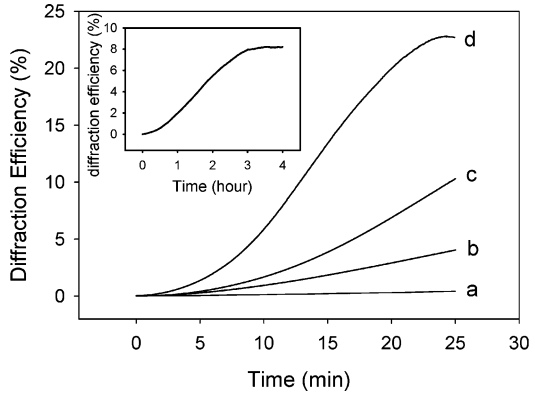

Figure 5. Diffraction efficiency curves for the photoformation of the SRGs with 1-μm spacing periods on (a) the PDO3 film with 500-nm thickness, and the amorphous TPPA films with thicknesses of (b) 200 nm, (c) 300 nm, and (d) 700 nm. Inset shows the diffraction efficiency on the PDO3 film monitored during irradiation for 4 h.

could be randomized in the dark through thermal processes such as cis to trans thermal isomerization and dipole redistribution to increase the entropy. These processes might proceed rapidly inside the TPPA films because of the lack of the cooperatively oriented polymer main chains.

To investigate and compare photoinduced SRG formation in the two materials, we exposed the amorphous TPPA and PDO3 films to an interference pattern of an Ar^+ laser beam with 50 mW/cm^2 intensity and monitored the diffraction efficiency at a wavelength of 633 nm using a He−Ne laser, as shown in Figure 5. After irradiation for 25 min, the diffraction efficiency of the TPPA film with a thickness of 300 nm reached 10%, but that of the PDO3 film with a thickness of 500 nm was only 0.4%. The diffraction efficiency of the TPPA film was proportional to the thickness of the film. For the 700-nm thick film, the diffraction efficiency reached 23% and then become saturated. Figure 6 shows a typical AFM image of the photofabricated SRGs with a spacing of 1 μm on the TPPA films. Regularly spaced and well-aligned relief structures can be seen. In this case, the diffraction efficiency was 16% and the surface modulation depth was 250 nm. When the same irradiation conditions were used for the PDO3 film with a thickness of 500 nm, the diffraction efficiency was 2% and the surface modulation depth was only 80 nm. The surface relief structures and the profiles of the TPPA molecular films were identical to the typically obtained SRG structures on the polymer films, and not much difference was found between the two types of the films in terms of uniformity and roughness.

Because of the faster increase in the diffraction efficiency and the higher SRG depth of the TPPA film compared to the PDO3 film, TPPA represents a potentially good holographic material and that could be used in fabricating optical elements. The origin of the rapid SRG photofabrication on the TPPA film might be the same as the reason for the fast growth of the photoinduced birefringence, i.e., the high azobenzene content per single molecule and the good mobility of the azobenzene groups due to the absence of polymer main-chains and their subsequent entanglement. However, our unpublished work suggests that the growth rate of photoinduced birefringence and SRG formation are

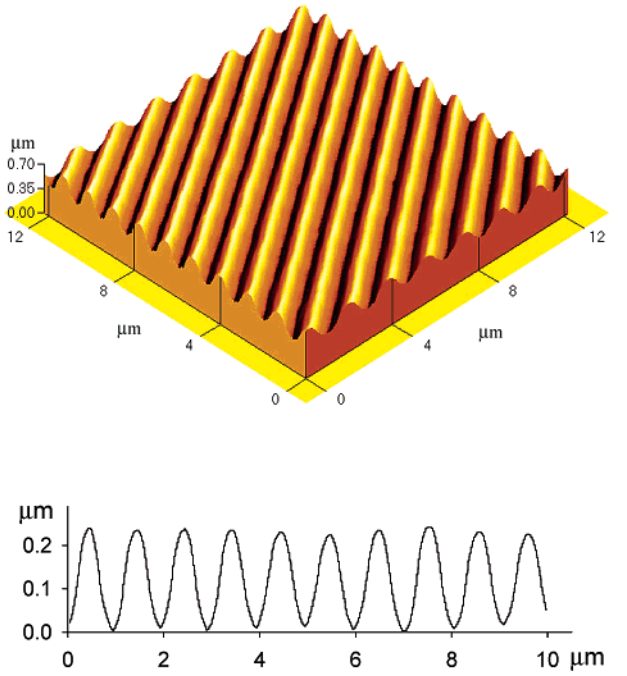

Figure 6. Typical 3-dimensional AFM image and depth profile of the SRGs on the amorphous TPPA film with 500-nm thickness at the diffraction efficiency of 16%. The surface modulation depth was 0.25 μm.

strongly dependent on the absorption wavelength of the azobenzene groups as well as the molecular weight. Therefore, at this time, we cannot generalize that all kinds of the azobenzene-functionalized molecular films would be more efficient than the polymeric films. To compare the characteristics of photoinduced behaviors between long chain polymer films and short chain molecular films more precisely, it would be necessary to compare azobenzene materials having the same composition, and, therefore, the same absorption wavelength, but with different molecular weights.

3.2. Comparison of SRG Formation between Amorphous and Semicrystalline Films of TPPA. Contrary to polymeric films, molecular films can be generally prepared by a vacuum deposition method. A unique property of the TPPA was its easy conversion into films by both spin-coating and vacuum deposition methods. Depending on the film preparation processes, the morphologies of the films can be varied, leading to different physical, chemical, and optical properties for the films. Therefore, we investigated the effect of film preparation methods on the photoformation of the SRGs in these two different types of films.

TPPA films with two different thicknesses of 150 and 300 nm were prepared by both methods and their UV−Vis absorption spectra were compared as shown in Figure 7. The maximum absorption wavelength (λ_{max}) and difference in λ_{max} ($\Delta\lambda_{max}$) depending on the film preparation method are also summarized in Table 2. Film thickness had no effect on the λ_{max} of the spin-coated films. However, the vacuum-deposited films showed different λ_{max} as the thickness changed. Furthermore, a thicker film (300 nm) showed some peaks in addition to the strong main absorption band. The λ_{max} of the spin-coated TPPA film with a 150 nm thickness was 443 nm (Figure 7a), but the λ_{max} of the vacuum-deposited TPPA film was red-shifted by 18 nm (Figure

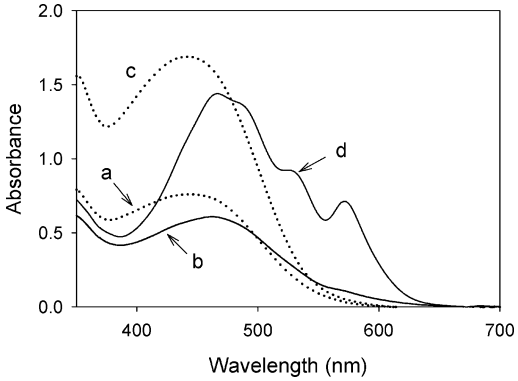

Figure 7. UV−Vis spectra of the spin-coated (dotted line) and vacuum-deposited (solid line) TPPA films. The thickness of the film was 150 nm (a, b) and 300 nm (c, d).

Table 2. Characteristic UV−Vis Spectral Wavelength Maxima for the TPPA Films Shown in Figure 7

film thickness	λ_{max} (nm) spin-coated film	λ_{max} (nm) vacuum-deposited film	$\Delta\lambda_{max}$ (nm)[a]
150 nm	443	461	18
300 nm	442	466	24
		487	45
		527	85
		571	129

[a] $\Delta\lambda_{max} = \lambda_{max}$ (vacuum deposited film) $- \lambda_{max}$ (spin-coated film).

7b). In the case of the vacuum-deposited TPPA film with a 300-nm thickness, the λ_{max} of the main absorption peak was also red-shifted by 24 nm compared to the spin-coated sample, and three additional fine peaks appeared at 487, 527, and 571 nm (Figure 7d).

The red-shift in the absorption peak in the vacuum-deposited films could be correlated with the J-aggregation of the chromophores. It is generally accepted that there are three types of chromophore aggregation depending on the angle between the transition dipole moment and the stacking direction of the aggregate: J-, H- and Herringbone aggregation.[27] J-aggregation involves a head-to-tail type chromophore alignment and would be expected to lead to an allowed transition shifted to a lower energy level (red-shift). The opposite is the case of the card-packing type aggregation, so-called H-aggregation, which involves the parallel stacking of the transition dipole moment. H-aggregation has been frequently observed for Langmuir−Blodgett thin films of several azobenzenes with a linear rod shape, and is reported to inhibit the photoisomerization of azobenzenes.[28−30] However, in our case, the nonplanar starburst shape of the TPPA molecule caused by the triphenylamine moieties is believed to prevent card-packing type aggregation (H-aggregation) of the chromophores, thus favoring J-aggregation.[31]

Figure 8 shows X-ray diffraction patterns of the TPPA films. The absence of a diffraction peak is evidence of an amorphous morphology in the spin-coated TPPA film (Figure 8a). However, the strong peak at $2\theta = 3.37°$ ($d = 26$ Å) is indicative of a crystalline morphology for the vacuum-deposited TPPA films, which probably exists as a head-to-tail type molecular arrangement. The d spacing of 26 Å is close to the diameter of the TPPA molecule. This also suggests the head-to-tail alignment of the molecules, consistent with the observation of a red-shift in the UV−Vis absorption spectra. The extent of crystallinity was strongly dependent on film thickness. The peak intensity of the 300-nm-thick film was 4.2 times larger than that of the 150-nm-thick film, indicating that thicker films possess a much higher crystallinity. In addition, a second diffraction peak can be observed at $2\theta = 6.77°$. The d spacing of the second peak was 13 Å, exactly half the distance of the first diffraction peak, suggesting that the origin of the crystallinity is the layer-type stacking of TPPA molecules.

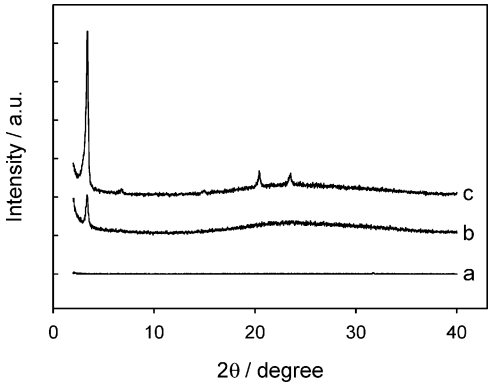

Figure 8. X-ray diffraction patterns of TPPA films prepared by spin-coating and vacuum deposition: (a) spin-coated TPPA film with a 300-nm thickness, and vacuum-deposited film with (b) a 150-nm thickness, and (c) a 300-nm thickness.

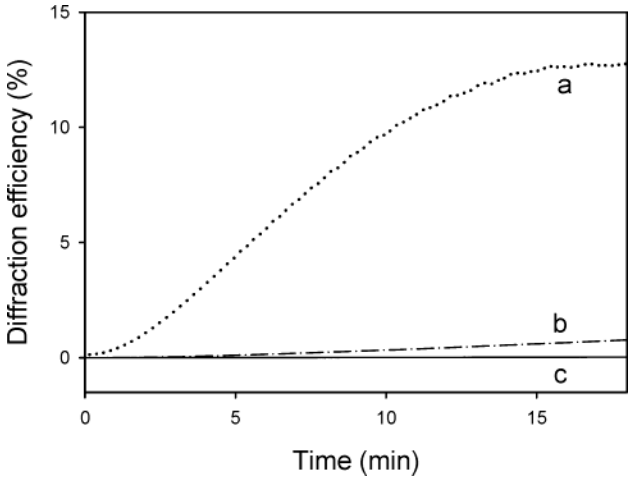

Figure 9. Diffraction efficiency curves for the photoinduced SRG formation as a function of the irradiation time on (a) the spin-coated TPPA film with 300-nm thickness and vacuum-deposited film with (b) 150-nm thickness, and (c) 300-nm thickness.

To investigate how the J-aggregated crystalline morphology affects photoinduced SRG formation, the spin-coated and vacuum-deposited TPPA films were exposed to an interference pattern of Ar^+ laser beams with a 100 mW/cm^2 intensity, and each diffraction efficiency curve was obtained, as shown in Figure 9. The diffraction efficiency increased rapidly up to 12% after irradiation for 15 min in the case of the spin-coated TPPA film

(27) Ramamurthy, V., Schanze, K. S., Eds. *Organic and Inorganic Photochemistry*; Mercel Dekker: New York, 1998.
(28) Wang, R.; Yang, J.; Wang, H.; Tang, D.; Jiang, L.; Li, T. *Thin Solid Films* **1995**, *256*, 205.
(29) Shembekar, V. R.; Dhanabalan, A.; Talwar, S. S.; Contractor, A. Q. *Thin Solid Films* **1999**, *342*, 270.
(30) Dos Santos, D. S., Jr.; Mendonça, C. R.; Balogh, D. T.; Dhanabalan, A.; Cavalli, A.; Misoguti, L.; Giacometti, J. A.; Zilio, S. C.; Oliveira, O. N., Jr. *Chem. Phys. Lett.* **2000**, *317*, 1.
(31) An, B.-K.; Kwon, S.-K.; Jung, S.-D.; Park, S.-Y. *J. Am. Chem. Soc.* **2002**, *124*, 14410.

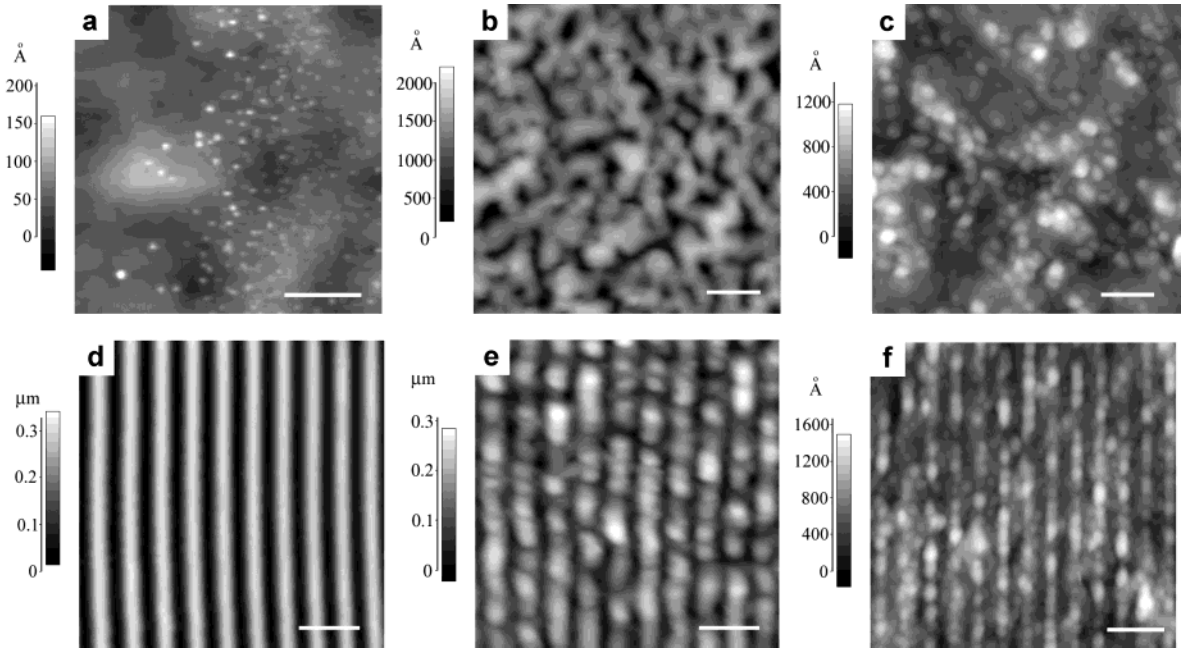

Figure 10. AFM images before (a−c) and after (d−f) photoinduced SRG formation on the spin-coated TPPA film with 300-nm thickness (a and d) and vacuum-deposited film with a 150-nm thickness (b and e), and a 300-nm thickness (c and f). (Scale bar, 2 μm).

with a 300-nm thickness (Figure 9a). However, for the vacuum-deposited films with a 150-nm thickness the diffraction efficiency increased only 0.6% for the same irradiation time. The obtained diffraction efficiency was almost zero for the vacuum-deposited TPPA film with a 300-nm thickness. Therefore, it would appear that an increase in crystallinity of the film prevents the mass transport required to form a surface grating structure.

Figure 10 shows the surface images of the TPPA films before and after SRG formation. The spin-coated TPPA film has a smooth and flat surface except for a few pinholes and defects (Figure 10a), but the vacuum-deposited film with a 150-nm thickness has a randomly grooved surface like a cerebral cortex with an average width of 1.2 μm (Figure 10b). In the surface of the vacuum-deposited film with 300-nm thickness, many aggregated spots were present whose average diameter was 0.8 μm (Figure 10c). After the TPPA films were exposed to the interference pattern, the depth of the photofabricated SRGs was 0.28 μm for the spin-coated TPPA film (Figure 10d), 0.18 μm for the vacuum-deposited film with a 150-nm thickness (Figure 10e), and 0.07 μm for the vacuum-deposited film with a 300-nm thickness (Figure 10f). The surface images of the groove and the aggregated spots on the films still remained on the surface of the SRG fabricated films. Therefore, we conclude that the vacuum deposition of the TPPA molecules induced a J-type aggregation or crystallinity and this led to the less efficient photoisomerization of azobenzene groups and subsequent molecular motions, thus inhibiting the fabrication of the SRGs.

4. Conclusions

A novel azobenzene-functionalized molecular glass was synthesized from triphenylamine-based precursor. Good optical quality amorphous films could be prepared by spin-coating and the resulting films showed a more rapid response to light than an azobenzene polymer PDO3 film in terms of the photoinduced birefringence and the photofabrication of SRGs. We also conclude that the photoinduced SRG formation was strongly dependent on conditions used in the preparation of the film. The crystalline morphology originating from molecular aggregation by the vacuum deposition process strongly prevented the photoformation of the SRG structures.

Acknowledgment. We thank Yong-Young Noh for preparing the vacuum vapor deposited films. This work was supported by the KOSEF (R01-2001-00324) and the Korea Energy Management Corporation.

CM034207D